15 February 1996

PHYSICS LETTERS B

ELSEVIER

Physics Letters B 369 (1996) 77–85

$\bar{p}p$ annihilation cross section at very low energy

OBELIX Collaboration

A. Bertin [a], M. Bruschi [a], M. Capponi [a], B. Cereda [a], S. De Castro [a], A. Ferretti [a], D. Galli [a], B. Giacobbe [a], U. Marconi [a], M. Piccinini [a], N. Semprini Cesari [a], R. Spighi [a], S. Vecchi [a], A. Vezzani [a], M. Villa [a], A. Vitale [a], A. Zoccoli [a], G. Belli [b], M. Corradini [b], A. Donzella [b], E. Lodi Rizzini [b], L. Venturelli [b], A. Zenoni [c], C. Cicalò [d], A. Masoni [d], G. Puddu [d], S. Serci [d], P. Temnikov [d], G. Usai [d], S. Costa [e,1], V.G. Ableev [f], O.Yu. Denisov [f], O.E. Gorchakov [f], S.N. Prakhov [f], A.M. Rozhdestvensky [f], M.G. Sapozhnikov [f], V.I. Tretyak [f], P. Gianotti [g], C. Guaraldo [g], A. Lanaro [g], V. Lucherini [g], F. Nichitiu [g,2], C. Petrascu [g,2], A. Rosca [g,2], C. Cavion [h], U. Gastaldi [h], M. Lombardi [h], L. Vannucci [h], G. Vedovato [h], A. Andrighetto [i], M. Morando [i], R.A. Ricci [i], G. Bendiscioli [j], V. Filippini [j], A. Fontana [j], P. Montagna [j], A. Rotondi [j], A. Saino [j], P. Salvini [j], A. Filippi [k], F. Balestra [ℓ], E. Botta [ℓ], T. Bressani [ℓ], M.P. Bussa [ℓ], L. Busso [ℓ], D. Calvo [ℓ], P. Cerello [ℓ], F. D'Isep [ℓ], L. Fava [ℓ], A. Feliciello [ℓ], L. Ferrero [ℓ], R. Garfagnini [ℓ], A. Grasso [ℓ], A. Maggiora [ℓ], S. Marcello [ℓ], N. Mirfakhraee [ℓ,3], D. Panzieri [ℓ], D. Parena [ℓ], E. Rossetto [ℓ], F. Tosello [ℓ], M. Agnello [m], F. Iazzi [m], B. Minetti [m], G. Pauli [n], S. Tessaro [n], L. Santi [o]

[a] *Dip. di Fisica, Università di Bologna and INFN, Sez. di Bologna, Bologna, Italy*
[b] *Dip. di Chimica e Fisica per i Materiali, Università di Brescia and INFN, Sez. di Torino, Italy*
[c] *Dip. di Chimica e Fisica per i Materiali, Università di Brescia and INFN, Sez. di Pavia, Italy*
[d] *Dip. di Scienze Fisiche, Università di Cagliari and INFN, Sez. di Cagliari, Cagliari, Italy*
[e] *CERN/PPE Geneva, Switzerland*
[f] *Joint Institute for Nuclear Research, Dubna, Russia*
[g] *Lab. Naz. di Frascati dell'INFN, Frascati, Italy*
[h] *Lab. Naz. di Legnaro dell'INFN, Legnaro, Italy*
[i] *Dip. di Fisica, Università di Padova and INFN, Sez. di Padova, Padova, Italy*
[j] *Dip. di Fisica Nucleare e Teorica, Università di Pavia and INFN, Sez. di Pavia, Pavia, Italy*
[k] *Dip. di Fisica Nucleare e Teorica, Università di Pavia and INFN, Sez. di Torino, Torino, Italy*
[ℓ] *Istituto di Fisica, Università di Torino and INFN, Sez. di Torino, Torino, Italy*
[m] *Dip. di Fisica, Politecnico di Torino and INFN, Sez. di Torino, Torino, Italy*
[n] *Ist. di Fisica, Università di Trieste and INFN, Sez. di Trieste, Trieste, Italy*
[o] *Ist. di Fisica, Università di Udine and INFN, Sez. di Trieste, Italy*

Received 4 December 1995
Editor: L. Montanet

SSDI 0370-2693(95)01599-X

Abstract

The $\bar{p}p$ total annihilation cross section has been measured, with the Obelix apparatus at LEAR, at ten values of the antiproton incident momentum between 43 and 175 MeV/c. The values of the cross section show that the well known $1/p$ behaviour of the annihilation cross section is drastically modified at very low momenta, which demonstrates the important role of the Coulomb force in low energy $\bar{p}p$ interaction. Moreover, they do not present any explicit resonant behaviour. Finally, when compared to potential model calculations, the data suggest that the percentage of P-wave in $\bar{p}p$ interaction around 50 MeV/c antiproton incident momentum is less than 5%.

1. Introduction

The value of the $\bar{p}p$ total annihilation cross section, at the lowest incident momentum reached so far (≈ 70 MeV/c), was measured [1] by the Obelix experiment [2] at LEAR. This was the first measurement performed by the experiment, with only a very limited part of the apparatus operational. Apart from this result, the $\bar{p}p$ cross sections were systematically measured only above 180 MeV/c incident momentum [3].

In the present paper, a new set of measurements of the $\bar{p}p$ total annihilation cross section, performed with the fully equipped spectrometer, is presented; the values of the cross section were obtained at several incident momenta: $174.4\pm2.0, 106.6\pm4.5, 65.1\pm2.0$, $63.6\pm2.0, 62.1\pm2.2, 60.5\pm2.2, 54.4\pm2.8, 52.9\pm2.8$, 51.3 ± 2.9 and 43.6 ± 3.1 MeV/c.

A particular effort was devoted to the measurement of the annihilation cross section at the lowest values of the incident momentum, for several reasons. First of all, a scan of the cross section at low values of the momentum, allows the possible existence of $\overline{N}N$ resonant and/or bound states near threshold, predicted by potential [4] and quark models [5], to be investigated. Second, the low energy $\overline{N}N$ cross sections can be analyzed, in a model independent way [6,7], in terms of the $\overline{N}N$ scattering length and effective range approximations and the $\overline{N}N$ scattering lengths can be extracted from the analysis.

Additionally, if at the lowest incident momenta the contribution of P-wave to the initial state angular momentum is verified to be less then some percent [8,9], the data taken in this condition could provide an effective means for selecting S-wave annihilations for meson spectroscopy studies [10–12]. In fact, annihilations at rest in liquid hydrogen are currently believed to be the best way to obtain annihilations in S-wave dominantly [13]. However, in this condition, the percentage of P-wave is at least 10% and is still matter of discussion [14,11]; moreover, the population of the singlet n^1S_0 and triplet n^3S_1 sublevels of the $\bar{p}p$ atom depend on the protonium electromagnetic cascade and are essentially unknown. On the contrary, in annihilations in flight, the protonium electromagnetic cascade is no longer involved and singlet and triplet S-wave contributions add incoherently with statistical spin factors [12].

Finally, if the partial cross sections for annihilation into specific final states could be measured as well, at low energy, as a function of the incident momentum, this would constitute a valuable input for quark model calculations of the annihilation process [8].

2. Experimental apparatus and data

Fig. 1 shows a sketch of the experimental layout: the incoming antiproton beam is degraded to a selected energy by the beryllium window of the beam pipe (100 μm), the thin scintillator of the beam counting system (C0) (100 μm scintillator plus 20 μm aluminized mylar) and by mylar foils of different thickness. Afterwards, the beam enters a hydrogen target (75 cm long and 30 cm diameter) whose pressure can be varied, from 10^{-4} bar to 3 bar absolute, in order to let the antiproton beam stop near or upon the end

[1] On leave of absence from Istituto di Fisica, Università di Torino, Torino, Italy.

[2] On leave of absence from Dep. of High Energy Physics, Inst. of Atomic Physics, Bucharest, Romania.

[3] On leave of absence from Shahid Beheshty University, Teheran, Iran.

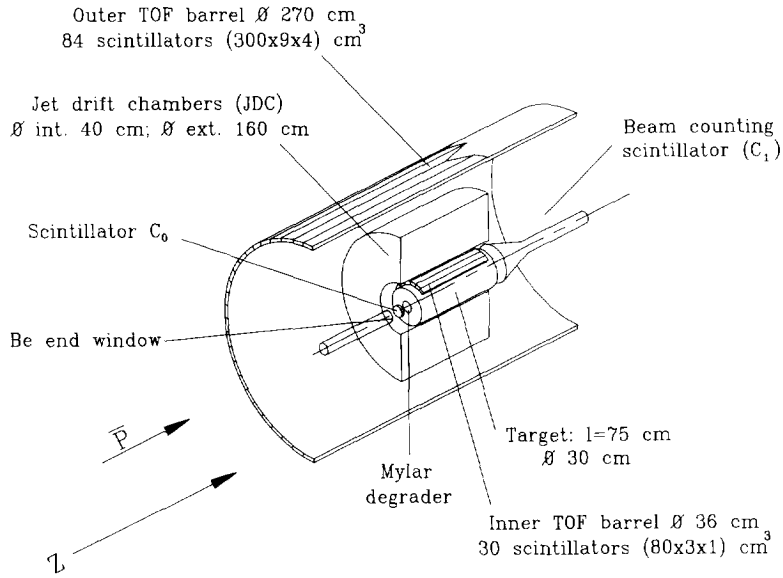

Fig. 1. Sketch of the experimental layout.

wall of the target.

Five different samples of data were recorded: at 201 MeV/c beam momentum setting, with a target gas pressure of 2.7 bar, two different degraders were used in order to obtain beam momenta of around 175 and 115 MeV/c at the entrance of the target; at 105 MeV/c beam setting, three different degraders were used in order to obtain beam momenta of around 70, 60, 50 MeV/c at the entrance of the target, with target pressures of 0.8, 0.5, 0.2 bar respectively.

The cross section for annihilation into charged products is measured by counting the number of annihilations in flight, occurring within a given fiducial volume inside the target, and the number of antiprotons crossing the target without interactions and annihilating at rest, near or upon its end wall.

The time at which the antiproton annihilations occur, starting from the beam counting scintillator (C0), increases with the longitudinal coordinate of the annihilation vertex along the beam/target axis (z coordinate). For the annihilations into charged particles, it is measured by the scintillator barrel placed around the target, hit by the charged products of the annihilation. At the trigger level, annihilations in flight are selected within a proper time gate ("event time gate") and recorded on tape; details about the time of flight system of the Obelix experiment can be found elsewhere [15]. The position of the vertices of the annihilation events is reconstructed by the system of two jet drift chambers of the Obelix spectrometer [2].

The beam crossing the target and annihilating on its end wall is counted, within another time gate ("beam time gate"), by detecting the hits of the charged products of the annihilation either in the same scintillator barrel mentioned above and/or in an additional scintillator disc (C1). This latter scintillator is positioned close to the end wall of the target and observed, through a long light guide, by a photomultiplier placed outside the magnet gap.

Since the incoming beam has been degraded in order to enter the target at a selected average energy, the beam momentum distribution is spread by the energy straggling. In order to recognize the annihilations inside the fiducial volume that are originated by different momentum components of the incoming beam, the data must be analyzed in a plot of the time of annihilation versus the z coordinate of the vertex.

Such a plot is shown in Fig. 2a, where the distribution of the data recorded at 0.8 bar is given; the plot is representative of the three samples recorded at 105 MeV/c beam setting. At these low energies the momentum of the antiprotons changes sensibly along the target and a careful analysis of the experimental data is necessary. To help in understanding the meaning

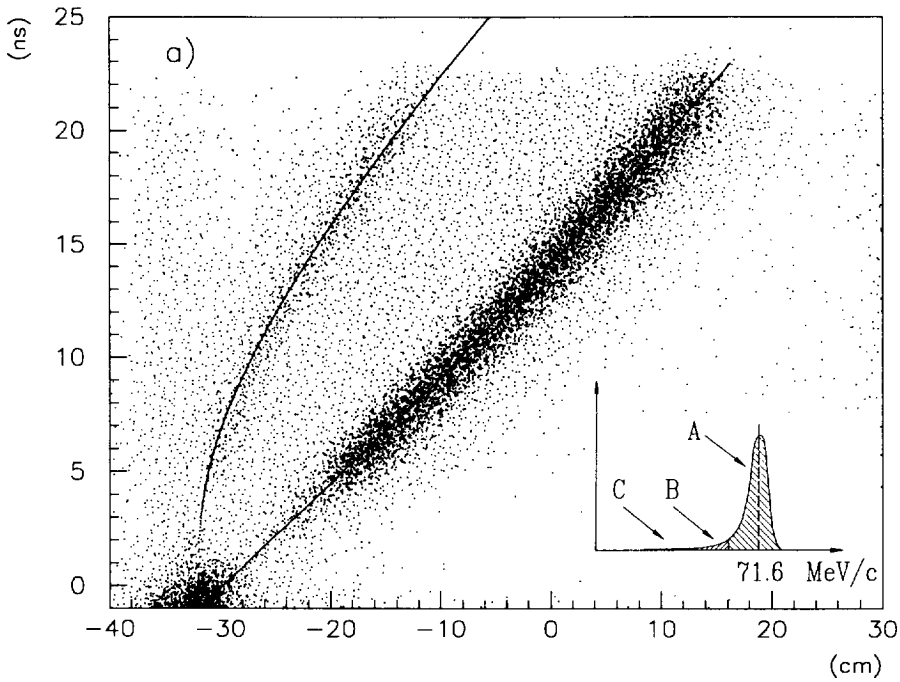

Fig. 2. a) Scatter plot of annihilation time versus z coordinate of the annihilation vertices for the sample at 0.8 bar, 105 MeV/c beam setting. b) "Lego plot" of the same distribution for time > 5 ns. In the inset of a) the shape of the beam momentum distribution at target entrance is suggested; for the meaning of A, B, C see text.

of the different structures seen in the scatter plot, the shape of the momentum distribution of the degraded beam at the entrance of the target is suggested in the inset of Fig. 2a.

It is worth reminding that the error on the determination of the z coordinate of the vertex of a single annihilation event is about 1 cm and the error in the annihilation time is about 1 ns. This latter error is due, in part, to the intrinsic time resolution of the internal scintillator barrel (0.5 ns) and, in part, to the fluctuation of the measurement of the time, due to the spread in time of flight of the first arriving charged product of the annihilation.

In the scatter plot two curved bands of accumulation of events are clearly seen. The lower band is due to annihilations in flight, at the average energy of the degraded beam (area A in the inset); the curvature of the band is the effect of the slowing down of the antiprotons in the gaseous target, the slope at each point being the average velocity of the antiprotons at the corresponding position in the target.

The upper band is due to the annihilations at rest of the antiprotons belonging to the low energy tail of the degraded beam (area C in the inset). This low energy tail constitutes a very small fraction of the beam entering the target; nevertheless it produces a significant signal, as every antiproton stopping inside the target, within the "event time gate", gives an annihilation which is recorded by the apparatus. On the contrary, annihilations in flight are generated by a small fraction ($\approx 10^{-3}$) of the antiprotons that cross the target.

The events between the two curved bands of annihilations in flight and at rest are due to annihilations in flight at energies lower than the average beam energy (areas B and C in the inset); events in other zones of the plot are due to inefficiencies of the timing system.

Annihilations on the degraders at the target entrance and on its end wall are largely the most probable. However they are not recorded, since they occur outside the "event time gate". Nevertheless, an accumulation of events belonging to the large number of annihilations on the degrader, at the target entrance, can be seen in the lower part of the picture; they are recorded by the apparatus owing to inefficiencies of the "event

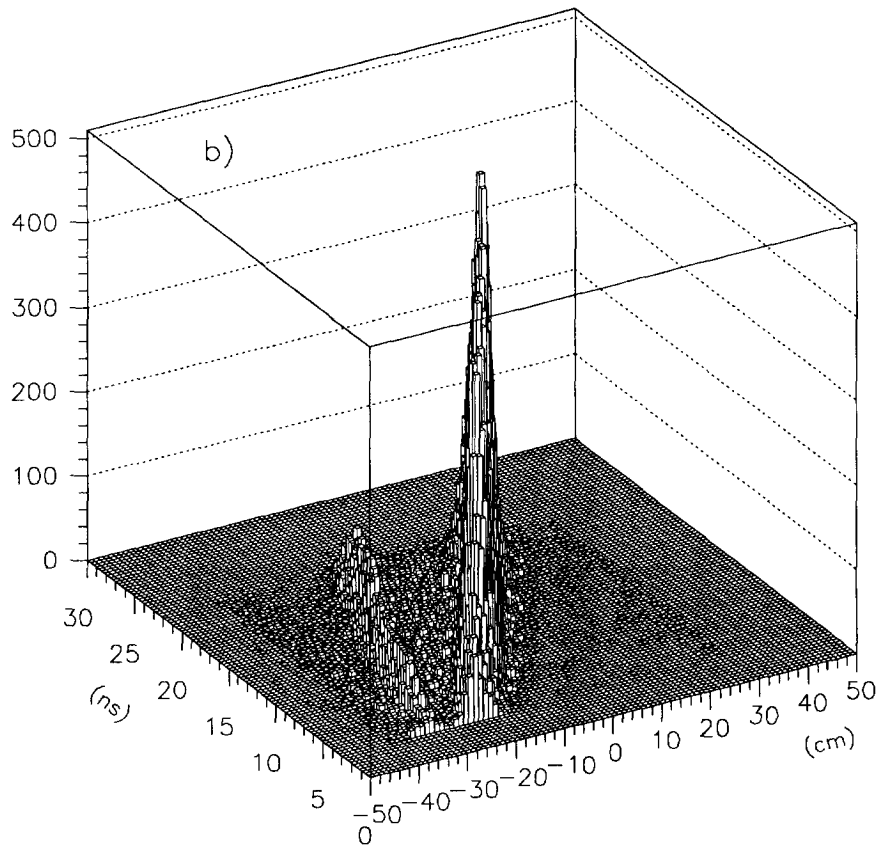

Fig. 2. Continued.

time gate".

The "Lego plot" of the time versus space distribution of Fig. 2a is shown in Fig. 2b; the relative proportions of the different components of the distribution are clearly evidenced in this representation. It is worth stressing that the separation of these different components is made possible, thanks to the capability of the Obelix apparatus to measure both the time of the annihilation and the position of the annihilation vertex.

The full lines superimposed on the two curved bands in Fig. 2a are the time versus space relationship, for the in flight events, and the stopping time versus range for the annihilations at rest. The two curves are calculated using the stopping power in gaseous hydrogen for low energy antiprotons, which was obtained by the Obelix experiment [16] by measuring range and time of moderation of the antiprotons in hydrogen targets at different densities.

The theoretical time versus space relationship, at the given target density, is fitted on the experimental distribution of in flight annihilations, leaving as free parameters the average beam momentum and the time, at the entrance of the target. The values of the average beam momenta at the entrance of the target, obtained from the fitting procedure, are respectively 71.6 ± 0.2, 60.2 ± 0.2 and 48.2 ± 0.2 MeV/c, at target pressures of 0.8, 0.5 and 0.2 bar. The errors on the momentum values are determined from the maximum uncertainty in the z coordinate of the entrance mylar window. For what concerns the time versus range relation, it is calculated for antiproton energies from zero to the average incoming beam energy, determined as above.

From Fig. 2 the theoretical predictions and the experimental data appear in good agreement. In particular, the time versus space relationship, superimposed to the in flight data, allows the value of the average

Table 1
$\bar{p}p$ total annihilation cross section at different antiproton incident momenta, multiplied by the velocity β of the antiprotons. In addition to the statistical and systematic errors, an overall normalization error of 3.4% has to be considered. Corresponding LEAR momentum settings, target pressures and average beam momenta at the entrance of the target are reported too.

LEAR beam (MeV/c)	target pressure (bar)	entrance momentum (MeV/c)	$\bar{p}$ incident momentum (MeV/c)	$\beta\sigma^T_{ann}$ (mbarn)
201	2.7	177.4 ± 1.0	174.4 ± 2.0	40.5 ± 0.5 (stat) ± 0.5 (sys)
„	„	116.6 ± 1.5	106.6 ± 4.5	40.4 ± 0.5 (stat) ± 1.7 (sys)
105	0.8	71.6 ± 0.2	65.1 ± 2.0	43.1 ± 0.7 (stat) ± 2.5 (sys)
„	„	„	63.6 ± 2.0	43.6 ± 0.7 (stat) ± 2.6 (sys)
„	„	„	62.1 ± 2.2	44.1 ± 0.7 (stat) ± 2.7 (sys)
„	„	„	60.5 ± 2.2	43.6 ± 0.7 (stat) ± 2.7 (sys)
„	0.5	60.2 ± 0.2	54.4 ± 2.8	46.0 ± 0.7 (stat) ± 2.4 (sys)
„	„	„	52.9 ± 2.8	46.4 ± 0.7 (stat) ± 2.5 (sys)
„	„	„	51.3 ± 2.9	47.0 ± 0.8 (stat) ± 2.7 (sys)
„	0.2	48.2 ± 0.2	43.6 ± 3.1	55.2 ± 0.9 (stat) ± 4.1 (sys)

momentum of the beam to be accurately determined for each value of the z coordinate.

For this reason, in the three sets of data recorded at 105 MeV/c beam setting, it was possible to sample the cross section at different values of the incident momentum inside the same target. This was done by selecting different fiducial volumes placed at increasing values of the z coordinate. Each fiducial volume corresponds to a different incident momentum, lower than the beam momentum at the entrance of the target. Four different fiducial volumes (which are cylinders of 10 cm radius and 4 cm length around the beam axis) were selected for the sample at 0.8 bar, three for the sample at 0.5 bar and one for the sample at 0.2 bar.

For the two samples recorded at the 201 MeV/c beam setting, the momentum of the antiproton changes slightly along the target; hence, the average beam momentum, in the center of the target, was simply obtained by fitting the complete time vs space distributions of in flight events with a straight line. The slope of this straight line gives the average velocity of the antiprotons. The values of the momentum at the entrance of the target are evaluated by accounting for the energy lost by the beam in crossing the target gas, from the entrance window to the center of the target; the values obtained are 177.4 ± 1.0 and 116.6 ± 1.5 MeV/c, where the errors account for both statistics and the procedure of averaging along the target length. For each sample, only one fiducial volume has been selected; in this case fiducial volumes are cylinders of 10 cm radius and 6 cm length around the beam axis.

A Monte Carlo calculation of the beam transport along the line provides the expected values of the beam momenta at the entrance of the target, in the different conditions: 176.4, 115.0 MeV/c and 70.7, 61.2, 49.5 MeV/c average entrance momenta at, respectively, 201 MeV/c and 105 MeV/c beam setting. The calculated values are in agreement within 2% with the values obtained from the fitting of the data. The corresponding expected values of the widths of the beam momentum distributions are the following: FWHM = 1.9, 7.0, 2.4, 4.0, 5.0 MeV/c.

In Table 1 the incident momentum values at the ten selected fiducial volumes, the corresponding average momenta at the entrance of the target, the target pressures and the momentum setting of the LEAR beam are reported. The errors on the values of the antiproton incident momenta are mainly determined by the lengths of the fiducial volumes and the widths of the beam momentum distributions estimated with the Monte Carlo simulation.

3. Values of the annihilation cross section

The values of the $\bar{p}p$ total annihilation cross section, at the different momenta of the incident antiprotons, are calculated following the formula :

$$\sigma^T_{ann} = \frac{N_{events}}{2 \cdot N_{\bar{p}} \cdot \rho \cdot \frac{N_A}{M} \cdot l \cdot \epsilon} \qquad (1)$$

where N_{events} is the number of in flight annihilation events reconstructed inside the given fiducial volume in the target, $N_{\bar{p}}$ is the number of antiprotons crossing the fiducial volume, ρ is the density of the target gas in g/cm^3, N_A is the Avogadro's number, M is the molecular weight of hydrogen, l is the length of the fiducial volume considered and ϵ is the efficiency of the apparatus for detecting events of $\bar{p}p$ annihilation. This last factor accounts also for the correction relative to the annihilation channels in all neutral particles, which cannot be detected by the apparatus.

The number of annihilations (N_{events}) is evaluated considering those events whose reconstructed vertices are within the given limits in z coordinate and radius and, in the time versus z plot, belong to the accumulation band of in flight events within 3σ's. Time projections of the z slices, in the time versus z planes, show that the times of in flight events, in the slices, are distributed as gaussians quite well.

The possible systematic error in the evaluation of N_{events} is estimated from the deviations of these time projections from a gaussian and is quite small. These deviations may originate from lower energy components of the beam. The systematic error, arising from the uncertainty in the measurement of z coordinate of the vertex, is compensated by the contribution of the target volumes neighboring the selected fiducial volume, whereas the error arising from the cut in radius is corrected by Monte Carlo simulation and is estimated to be quite small.

Possible sources of background arise both from the annihilations occurring at rest on the target walls, whose vertex is reconstructed inside the fiducial volume, and from the background due to inefficiencies of the timing system. The former contamination on N_{events} is evaluated using a sample of data recorded with an empty target, while the latter one is negligible, as it can be seen from the small number of counts above 3σ's in the lower part of the plot of Fig. 2a.

The number of antiprotons ($N_{\bar{p}}$) crossing the target is obtained from the number of annihilations counted within the "beam time gate", corrected for the efficiency of the beam counting system. This last correction factor has been both evaluated with a Monte Carlo simulation and measured from the data.

The efficiency (ϵ) for detection of annihilations events has been calculated with a Monte Carlo simulation of the apparatus; the simulation takes into account the shape of the vertex distribution, the average beam energy, the geometrical structure of the detectors and their detection efficiencies. The production rates for the most frequent annihilation channels in charged and neutral particles are set in order to correctly reproduce the experimental distribution of the charged topologies of the $\bar{p}p$ annihilation.

For what concerns the contribution of all neutral annihilation channels in the Monte Carlo simulation, it amounts to 2.9% and 4.1% for the samples recorded, respectively, at 201 MeV/c and 105 MeV/c incident momentum. This assumption is justified by the value of the fractions of annihilations into all neutral particles measured at rest in a gaseous target at NTP [17] $(2.9\pm0.5)\%$ and in liquid hydrogen [18] $(4.1^{+0.2}_{-0.6})\%$. In fact, for what concerns the mixing of the initial state orbital angular momenta, these two conditions are the most similar, respectively, to in flight annihilations around 150 MeV/c and to in flight annihilations at very low energy; in the former case S- and P-waves should contribute in the same fraction [8], whereas in the latter one S-wave should be dominant.

Table 1 reports the values of the total annihilation cross section at the different incident momenta (as obtained from formula (1)), multiplied by the velocity β of the incoming antiproton. The systematic errors of the cross section values are obtained as the quadratic addition of two possible systematic uncertainties: one connected with the determination of the antiproton interaction momentum and the other with the determination of the number of annihilation events occurring inside the fiducial volume. For the sample recorded at 0.8 bar, a further systematic uncertainty arises from the correction of the beam flux, due to an accidental wrong setting of the "beam time gate". Apart from this particular case, the systematic error on the $\beta\sigma^T_{\text{ann}}$ values is dominated by the uncertainty in the antiproton incident momentum, due to the energy straggling in beam degradation.

In addition to the systematic error, an overall normalization error of 3.4% has to be considered for both the samples recorded at 201 MeV/c and 105 MeV/c beam setting. It arises from the quadratic addition of the uncertainties on different corrections: the Monte Carlo correction for apparatus efficiency, the correction for annihilations in all neutral particles as well as the correction for the beam counting efficiency. The possible uncertainty in the determination of the gas

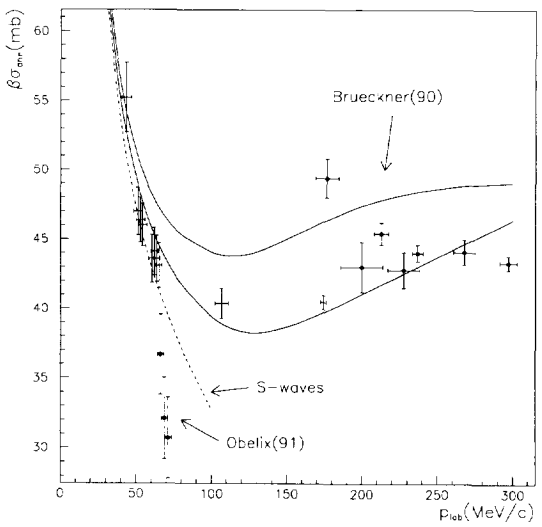

Fig. 3. Values of the total $\bar{p}p$ annihilation cross section at low energy multiplied by the incoming beam velocity. Measurements from Brückner et al. [3] and Obelix [1] are reported too. Theoretical curves are from a CCM model of Carbonell et al. [19]. Full lines are total annihilation cross sections, the dashed line represents the S-wave contribution for both parametrizations.

density is accounted too in the overall normalization factor.

4. Results and discussion

In Fig. 3 the values of $\beta\sigma^T_{\rm ann}$ from Table 1 are plotted versus the antiproton momentum. The reported error bars represent the quadratic addition of the statistical error and the systematic error interval divided by $\sqrt{12}$. In the picture, the values of $\beta\sigma^T_{\rm ann}$ measured by Brückner et al. [3] at higher energies and by Obelix [1] around 70 MeV/c, are reported too for comparison. The full curves superimposed to the data are the predictions, for the total annihilation cross section, from two different parameterization of a CCM model from Carbonell et al. [19]; the dashed line represents the contribution of S-waves for both parametrizations. In the model, the effect of the Coulomb interaction on the annihilation process is accounted for.

The comparison of the present measurements of $\beta\sigma^T_{\rm ann}$ with the previous ones from Brückner et al. [3] shows that the point at 176.8 MeV/c from Brückner et al. [3] is incompatible with the Obelix result at approximately the same momentum. The cross section values remain incompatible even if the overall normalization error of the latter data, which is 4.4%, is taken into account. On the contrary, the absolute values and the behaviour of the other points seem to be well connected with the new determinations of the cross section.

Concerning the previous results of Obelix [1] around 70 MeV/c incident momentum, they are clearly underestimated when compared to the new determinations of $\beta\sigma^T_{\rm ann}$. Nevertheless, the behaviour of the three points, which is increasing with decreasing the value of the momentum, is the same as in the present data. The reason for this disagreement can be attributed to the fact that only a limited part of the apparatus was used to detect the annihilations in the previous measurement. Therefore, a much larger Monte Carlo correction was necessary, while the understanding of the efficiency of the different detectors was much less accurate than in the present one.

Hence, evidently, the systematic error was larger than previously estimated. Unfortunately, since in the present measurement at 105 MeV/c beam setting the set up was optimized to measure the cross section at momenta lower than 65 MeV/c, it was not possible to make a new determination of the cross section around 70 MeV/c.

Concerning the behaviour of the $\bar{p}p$ annihilation cross section at very low energy, it is evident that the well known $1/p$ law of the annihilation cross section is drastically modified. This demonstrates the important role of the Coulomb force in low energy $\bar{p}p$ interaction; indeed, the $\bar{p}p$ Coulomb potential creates a divergence of $\beta\sigma^T_{\rm ann}$ at zero energy [9]. Additionally, no apparent resonant behaviour is shown by the measured values of the $\bar{p}p$ cross section.

The comparison of the data with the theoretical predictions from a CCM model of Carbonell et al. [19] shows that the values of the cross section are in agreement with the prediction of the model, at least in one of the two parametrizations. However, around 50 MeV/c, the model seems to overestimate the contribution of the P-waves to the annihilation cross section (in the model this contribution amounts to 4.5% at that energy). On the contrary, the model seems to underestimate the value of the cross section at the lowest momentum value of 43.6 MeV/c. Considering that this point is affected by a large error, further measure-

ments of the cross section at these very low energies should be performed, in order to clarify the nature of this discrepancy.

References

[1] M. Agnello et al., Phys. Lett. B 256 (1991) 349.
[2] A. Adamo et al., Sov. J. Nucl. Phys. 55 (11) (1992) 1732.
[3] W. Brückner et al., Phys. Lett. B 169 (1986) 302; B 166 (1986) 113; Z. Phys. A 335 (1990) 217; A 339 (1991) 367.
[4] I.S. Shapiro, Phys. Rep. C 35 (1978) 129;
W.W. Buck, C.B. Dover and J.M. Richard, Ann. Phys. (NY) 121 (1979) 47, 70;
M. Lacombe et al., Phys. Rev. C 29 (1984) 1800;
O.D. Dalkarov, K.V. Protasov and I.S. Shapiro, Int. J. Mod. Phys. A 5 (5) (1990) 2155.
[5] R.L. Jaffe, Phys. Rev. D 15 (1977) 267, 281; D 17 (1978) 1445;
Chan Hong Mo and H. Högaasen, Nucl. Phys. B 136 (1978) 401; Phys. Lett. B 76 (1978) 634.
[6] J. Mahalanabis, H.J. Pirner and T.A. Shibata, Nucl. Phys. A 485 (1988) 546.
[7] A.E. Kudryavtsev and B.L. Druzjinin, ITEP Preprint 23-94 (1994).
[8] C.B. Dover et al., Prog. Part. Nucl. Phys. B 29 (1992) 219.
[9] J. Carbonell and K.V. Protasov, Hyp. Inter. 76 (1993) 327.
[10] E. Lodi Rizzini, Riv. Nuovo Cim. 15 (1992) 1.
[11] A. Rotondi, Nucl. Phys. A 558 (1993) 235c.
[12] A. Zenoni, LEAP'94 – Third Biennal Conference on Low Energy Antiproton Physics (Bled, Slovenia Sep. 1994), eds. G. Kernel et al. (World Scientific, 1995) p. 242.
[13] C.J. Batty, Rep. Prog. Phys. 52 (1989) 1165.
[14] U. Gastaldi et al., Phys. Lett. B 320 (1994) 193.
[15] G.C. Bonazzola et al., Nucl. Instr. Meth. A 356 (1995) 270.
[16] A. Adamo et al., Phys. Rev. A 47 (1993) 4517;
M. Agnello et al., Phys. Rev. Lett. 74 (1995) 371.
[17] J. Riedelberg et al., Phys. Rev. C 40 (1989) 2717.
[18] C. Ghesquiere, Symp. on Antinucleon-Nucleon Interaction Liblice, (1974); CERN 74-18, p. 486.
[19] J. Carbonell, private communication;
O.D. Dalkarov, J. Carbonell, K.V. Protasov, Sov. J. Nucl. Phys. 52 (1990) 1052.